Factors Modulating the Hydrolysis of Nylon-6,6 by a Nylon Hydrolase Enzyme

Vera Bocharova[1,†], Erin E. Drufva[2], John F. Cahill[2], Ivan Popov[3], Isaiah T. Dishner[1], Muchu Zhou[1], Gang Seob Jung[4], Andrew M. Ullman[1], Dana L. Carper[2], Joshua T. Damron[1], Jong K. Keum[5,6], Catalan Gainaru[1], Serena H. Chen[4], Jeffrey C. Foster[1,†], Joshua K. Michener[2,†]

[1]Chemical Sciences Division, Oak Ridge National Laboratory, Oak Ridge, TN 37831, USA

[2]Biosciences Division, Oak Ridge National Laboratory, Oak Ridge, TN 37831, USA

[3] University of Tennessee-Oak Ridge Innovation Institute, University of Tennessee, Knoxville, TN 37996, USA

[4]Computational Sciences and Engineering Division, Oak Ridge National Laboratory, Oak Ridge, TN 37831, USA

[5]Center for Nanophase Materials Science, Oak Ridge National Laboratory, Oak Ridge, TN 37831, USA

[6]Neutron Scattering Division, Oak Ridge National Laboratory, Oak Ridge, TN 37831, USA

†Corresponding authors: Vera Bocharova (bocharovav@ornl.gov), Jeffrey C. Foster (fosterjc@ornl.gov), Joshua K. Michener (michenerjk@ornl.gov)

Synthesis of L1

Synthesis of Methyl 6-[[6-[[(t-butoxy)carbonyl]amino]hexyl]amino]- 6-oxohexanoate: A 1000 mL RBF was charged with monomethyl adipate (7.5 g, 46.8 mmol, 1 equiv.) and 450 mL dichloromethane (DCM). EDC·HCl (9.87 g, 51.5 mmol, 1.1 equiv.) was added and the RBF was stirred at r.t. for 5 min until dissolved. N-Boc-1,6-hexamethylenediamine (11.15 g, 51.5 mmol, 1.1 equiv) was then added to the reaction mixture and the reaction was stirred at r.t. overnight. The reaction was washed with 2×250 mL 1 M HCl, 3×250 mL mL saturated $NaHCO_3$ solution, and 250 mL brine. The organic layer was dried over sodium sulfate, filtered, and concentrated using a rotary evaporator. The product (11.02 g, 66%) was dried overnight in a vacuum oven and used in subsequent reactions without further purification. ^{1}H NMR (400 MHz, $CDCl_3$) δ 5.71 (s, 1H), 4.55 (s, 1H), 3.66 (s, 3H), 3.22 (td, *J* = 7.0, 5.8 Hz, 2H), 3.10 (q, *J* = 6.7 Hz, 2H), 2.39 – 2.25 (m, 2H), 2.18 (dq, *J* = 6.7, 3.5 Hz, 2H), 1.84 – 1.57 (m, 5H), 1.43 (s, 13H), 1.32 (p, *J* = 3.9 Hz, 4H). ^{13}C NMR (101 MHz, $CDCl_3$) δ 174.14, 172.61, 156.23, 79.18, 51.70, 40.27, 39.22, 36.44, 33.81, 30.11, 29.56, 28.54, 26.30, 26.15, 25.26, 24.54.

Synthesis of 6-[[6-[[(t-butoxy)carbonyl]amino]hexyl]amino]-6-oxohexanoic acid: To a solution of Methyl 6-[[6-[[(1,1-dimethylethoxy)carbonyl]amino]hexyl]amino]- 6-oxohexanoate (11 g, 30.6 mmol) dissolved in tetrahydrofuran (THF) (110 mL) was added 1 M LiOH (110 mL). The reaction was stirred for 3.5 h, and subsequently acidified to pH 4 with 1 M HCl. This solution was concentrated via rotary evaporation, and the white precipitate was filtered to provide the corresponding carboxylic acid in quantitative yield. ^{1}H NMR (400 MHz, DMSO) δ 12.01 (s, 1H), 7.75 (t, *J* = 5.7 Hz, 1H), 6.77 (t, *J* = 5.7 Hz, 1H), 3.00 (q, *J* = 6.6 Hz, 2H), 2.88 (q, *J* = 6.6 Hz, 2H), 2.19 (t, *J* = 6.9 Hz, 2H), 2.04 (t, *J* = 6.8 Hz, 2H), 1.57 – 1.41 (m, 4H), 1.37 (s, 13H), 1.23 (dt, *J* =

7.7, 3.8 Hz, 4H). ^{13}C NMR (101 MHz, DMSO) δ 174.92, 172.12, 156.04, 77.75, 40.16, 38.78, 35.58, 33.96, 29.91, 29.61, 28.74, 26.59, 26.47, 25.35, 24.63.

Synthesis of 6-[(6-Aminohexyl)amino]-6-oxohexanoic acid trifluoroacetate (L1 TFA salt): In a 500 mL RBF, 6-[[6-[[(1,1-dimethylethoxy)carbonyl]amino]hexyl]amino]-6-oxohexanoic acid (10 g, 29 mmol) was suspended in DCM (150 mL). The RBF was chilled to 0 °C in an ice bath and trifluoroacetic acid (50 mL) was added slowly to the reaction. The flask was stirred overnight, warming gradually to room temperature. The majority of trifluoroacetic acid was removed by concentrating the reaction *in vacuo* and rediluting with DCM (150 mL) for 3 cycles. After the third cycle, the concentrated crude was precipitated into diethyl ether (100 mL). The ether layer was decanted and the product was dried under vacuum to provide the product as a viscous yellow oil (8.46 g, 81%). ^{1}H NMR (400 MHz, D_2O) δ 3.14 (t, J = 6.8 Hz, 2H), 2.94 (t, J = 7.6 Hz, 2H), 2.44 – 2.30 (m, 2H), 2.21 (td, J = 6.7, 4.1 Hz, 2H), 1.70 – 1.21 (m, 12H). ^{13}C NMR (101 MHz, MeOD) δ 177.28, 175.81, 163.18, 119.66, 40.60, 40.01, 36.71, 34.56, 30.14, 28.43, 27.30, 26.95, 26.50, 25.54.

Synthesis of 6-[(6-Aminohexyl)amino]-6-oxohexanoic acid (L1): Reillex 402 (11.73 g, 112 meq) was added to a stirred solution of trifluoroacetate salt (8 g, 22.3 mmol) dissolved in deionized water (80 mL) and stirred overnight. The reaction was filtered and the filtrate was concentrated *in vacuo* to provide a yellow residue that was further purified by triturating with ethanol. The product was isolated as a white powder (3.28 g, 60%). ^{1}H NMR (400 MHz, D_2O) δ 3.05 (t, J = 6.7 Hz, 2H), 2.84 (t, J = 7.6 Hz, 2H), 2.11 (t, J = 6.8 Hz, 2H), 2.05 (t, J = 7.0 Hz, 2H), 1.67 – 1.31 (m, 8H), 1.31 – 1.09 (m, J = 5.5, 4.1 Hz, 4H). ^{13}C NMR (101 MHz, D_2O) δ 183.28, 176.64, 39.30, 38.91, 37.11, 35.54, 27.91, 26.54, 25.34, 25.33, 25.16, 25.09.

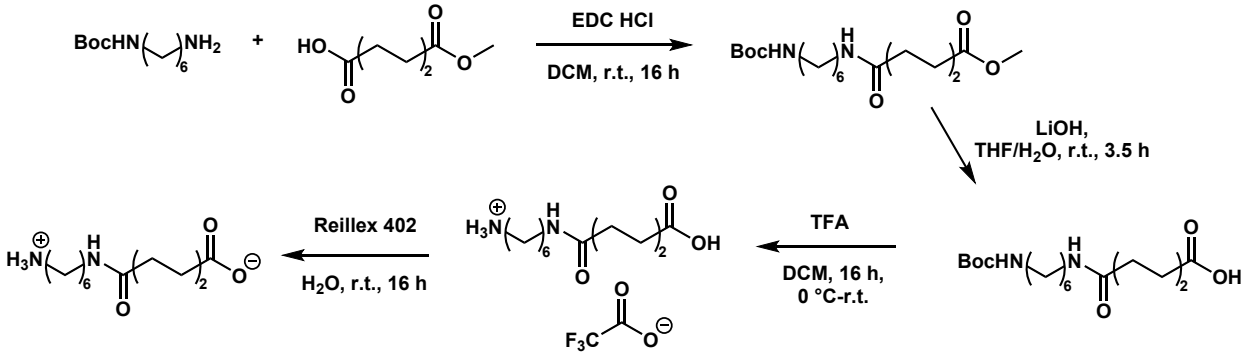

Scheme S1. Synthesis of **L1**.

MNTTPVHALTDIDGGIAVDPAPRLAGPPVFGGPGNAAFDLAPVRSTGREMLRFDFPGVSI
GAAHYEEGPTGATVIHIPAGARTAVDARGGAVGLSGGYDFNHAICLAGGAGYGLEAGA
GVSGALLERLEYRTGFAELQLVSSAVIYDFSARSTAVYPDKALGRAALEFAVPGEFPQG
RAGAGMSASAGKVDWDRTEITGQGAAFRRLGDVRILAVVVPNPVGVIVDRAGTVVRG
NYDAQTGVRRHPVFDYQEAFAEQVPPVTQAGNTTISAIVTNVRMSPVELNQFAKQVHS

SMHRGIQPFHTDMDGDTLFAVTTDEIDLPTTPGSSRGRLSVNATALGAIASEVMWDAVL
EAGK

Scheme S2. The complete amino acid sequence for NylC-GYAQ .

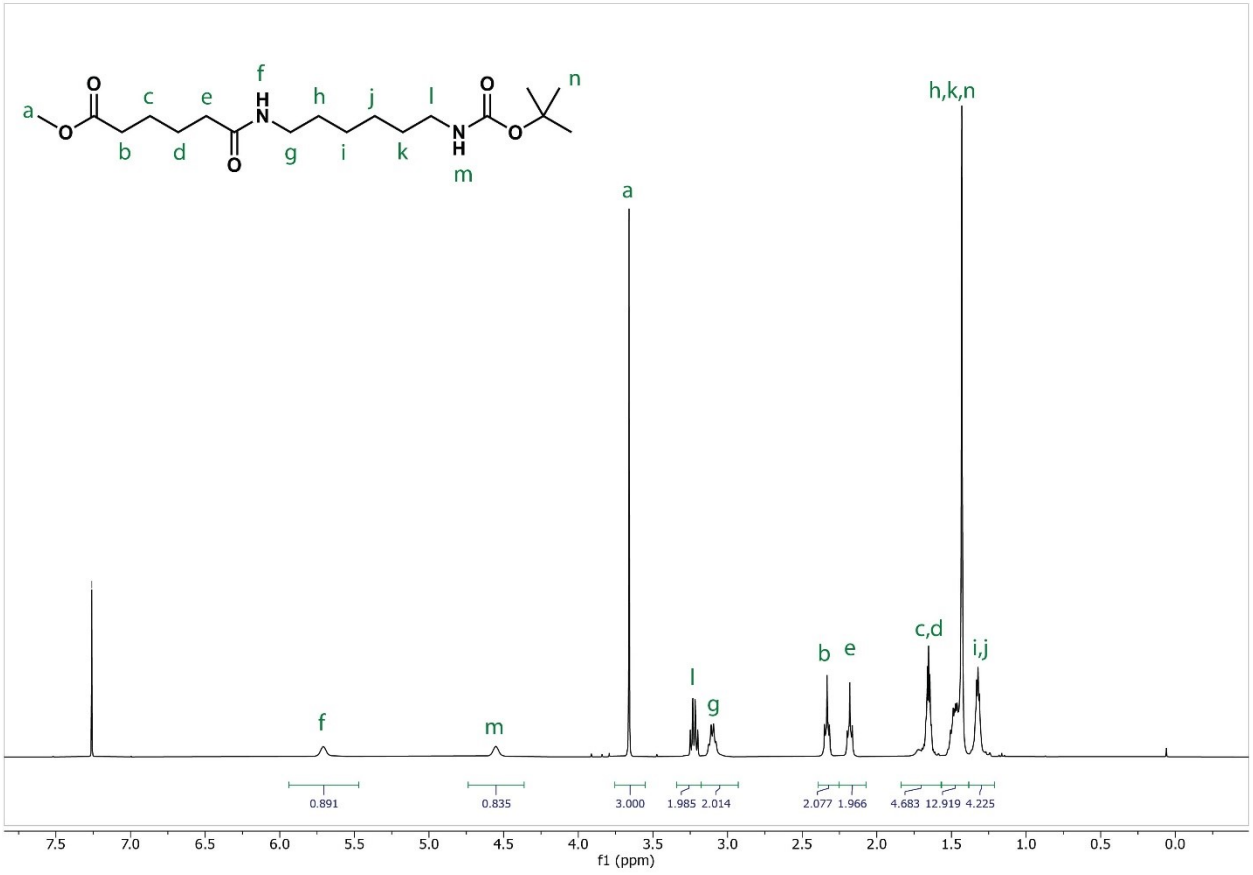

Figure S1. ^{1}H NMR spectrum of methyl 6-[[6-[[(*t*-butoxy)carbonyl]amino]hexyl]amino]- 6-oxohexanoate collected in $CDCl_3$.

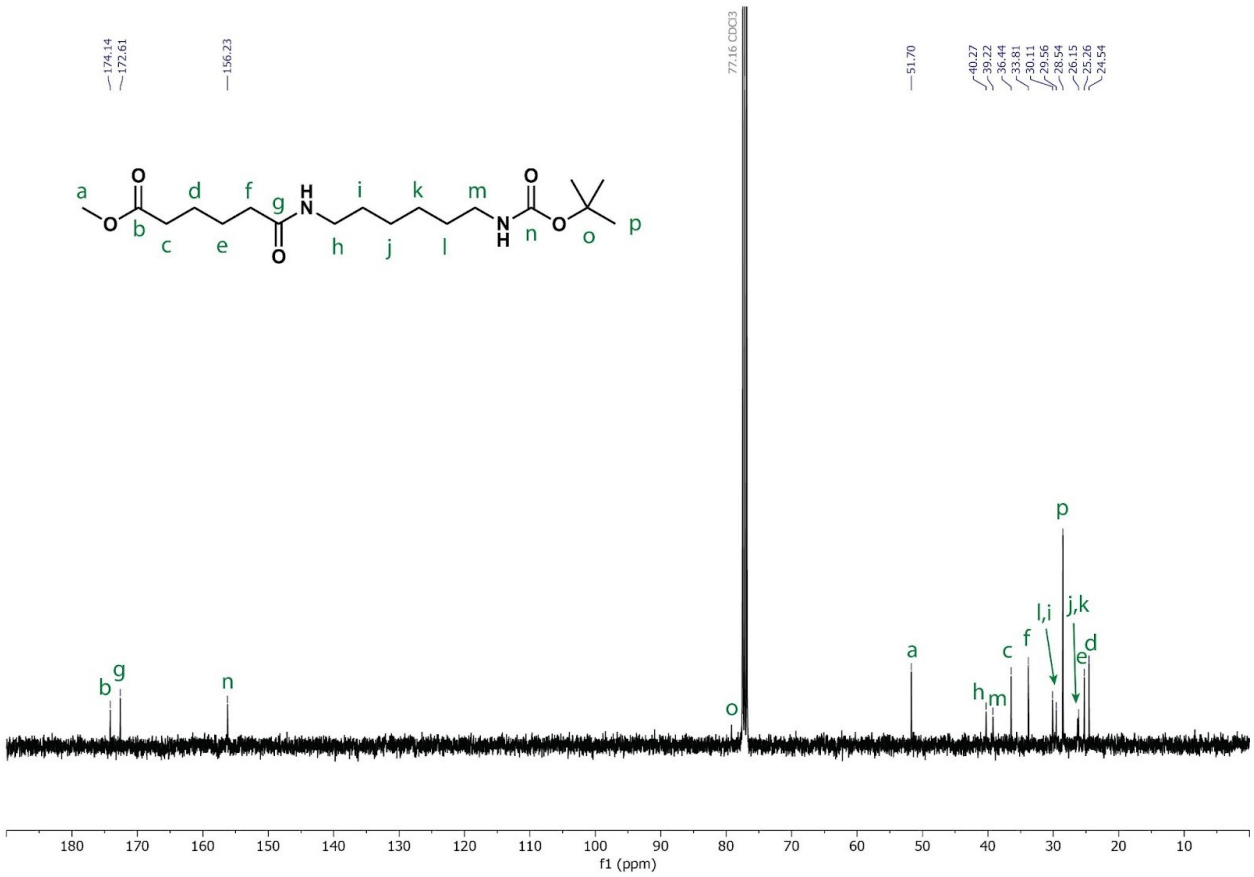

Figure S2. ^{13}C NMR spectrum of methyl 6-[[6-[[(*t*-butoxy)carbonyl]amino]hexyl]amino]- 6-oxohexanoate collected in $CDCl_3$.

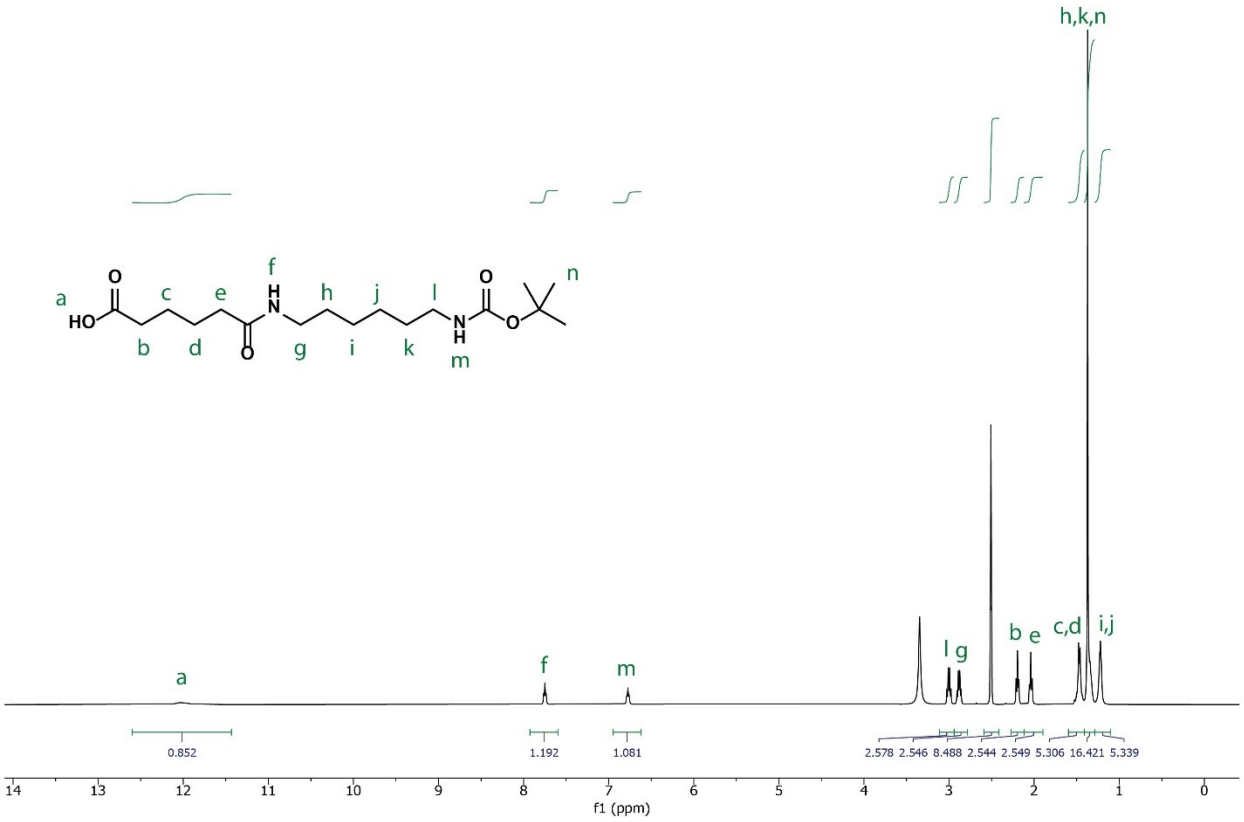

Figure S3. ^{1}H NMR spectrum of 6-[[6-[[(*t*-butoxy)carbonyl]amino]hexyl]amino]-6-oxohexanoic acid collected in DMSO-d_6.

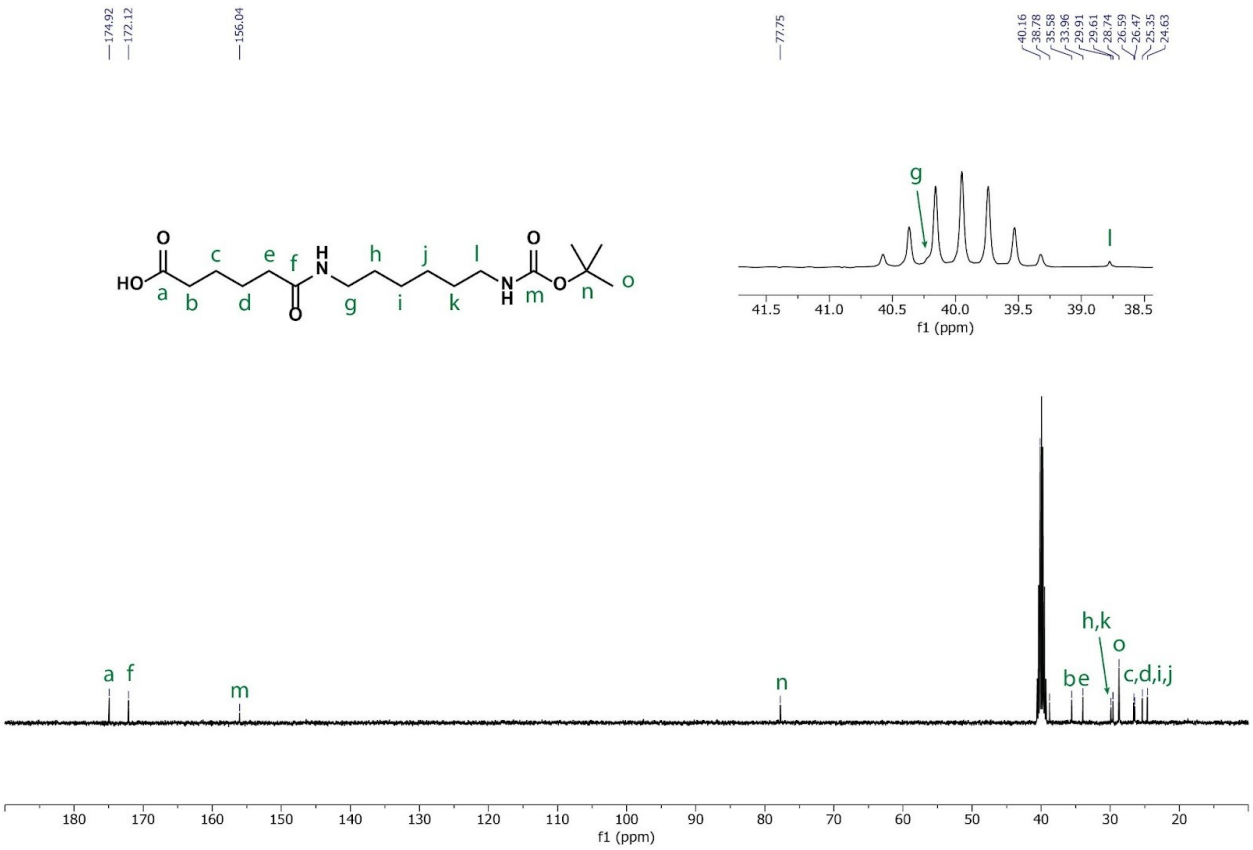

Figure S4. ^{13}C NMR spectrum of 6-[[6-[[(*t*-butoxy)carbonyl]amino]hexyl]amino]-6-oxohexanoic acid collected in DMSO-d_6.

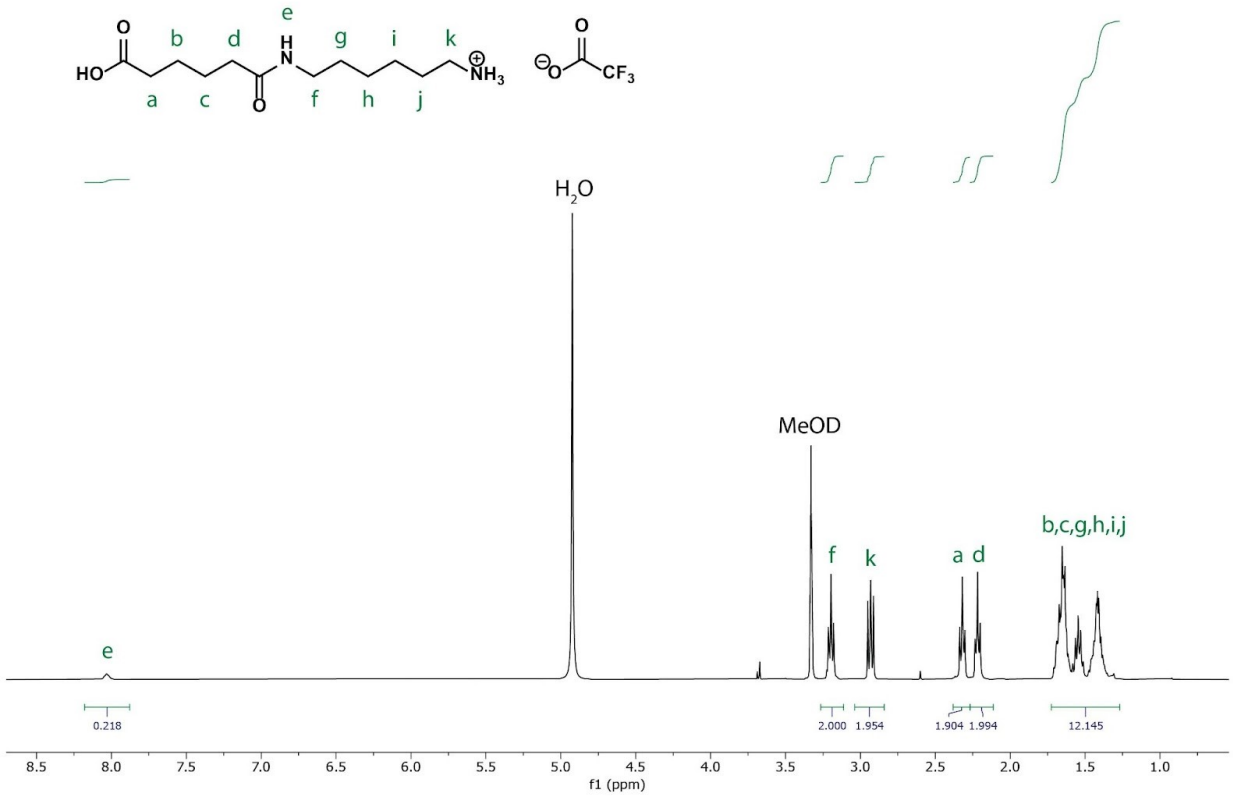

Figure S5. ^{1}H NMR spectrum of MA TFA salt in MeOD.

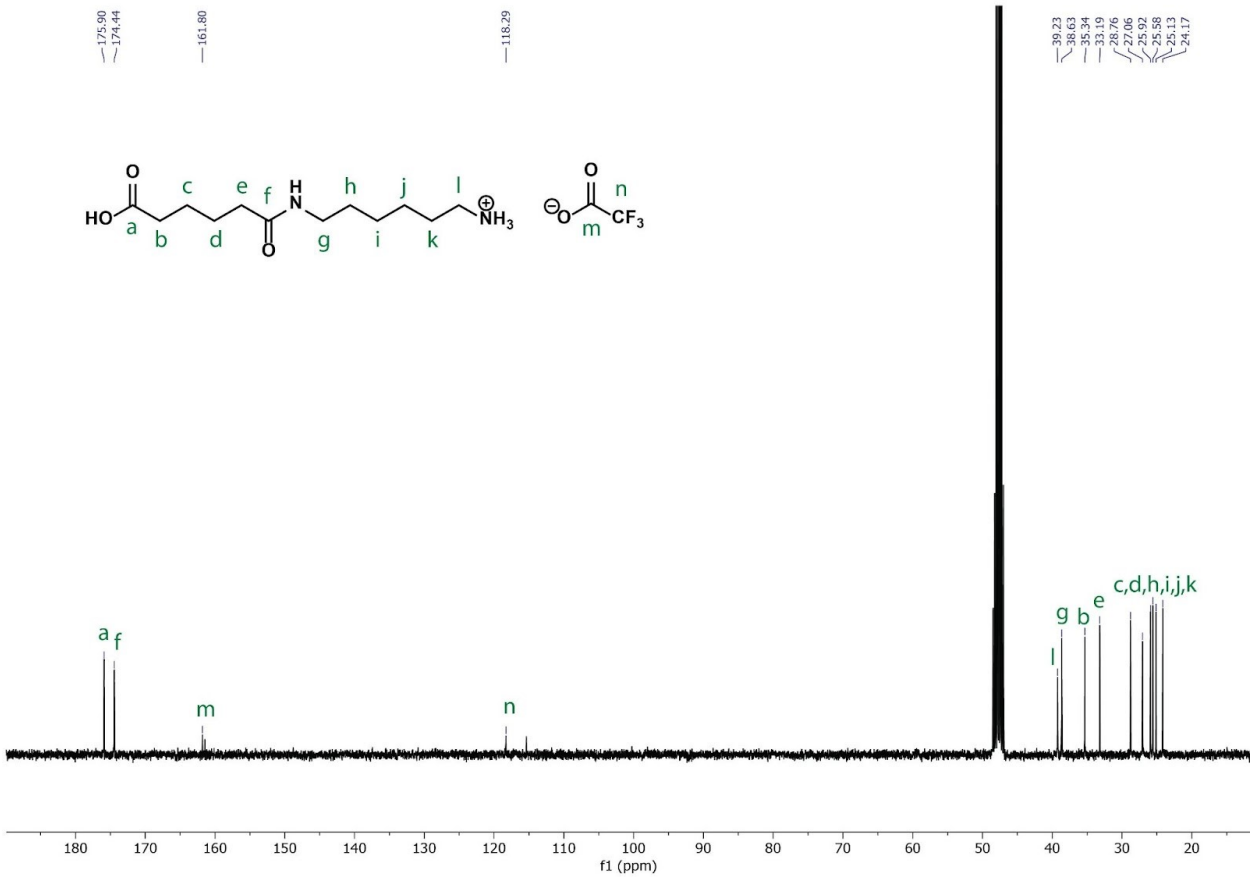

Figure S6. ^{13}C NMR spectrum of L1 TFA salt in MeOD.

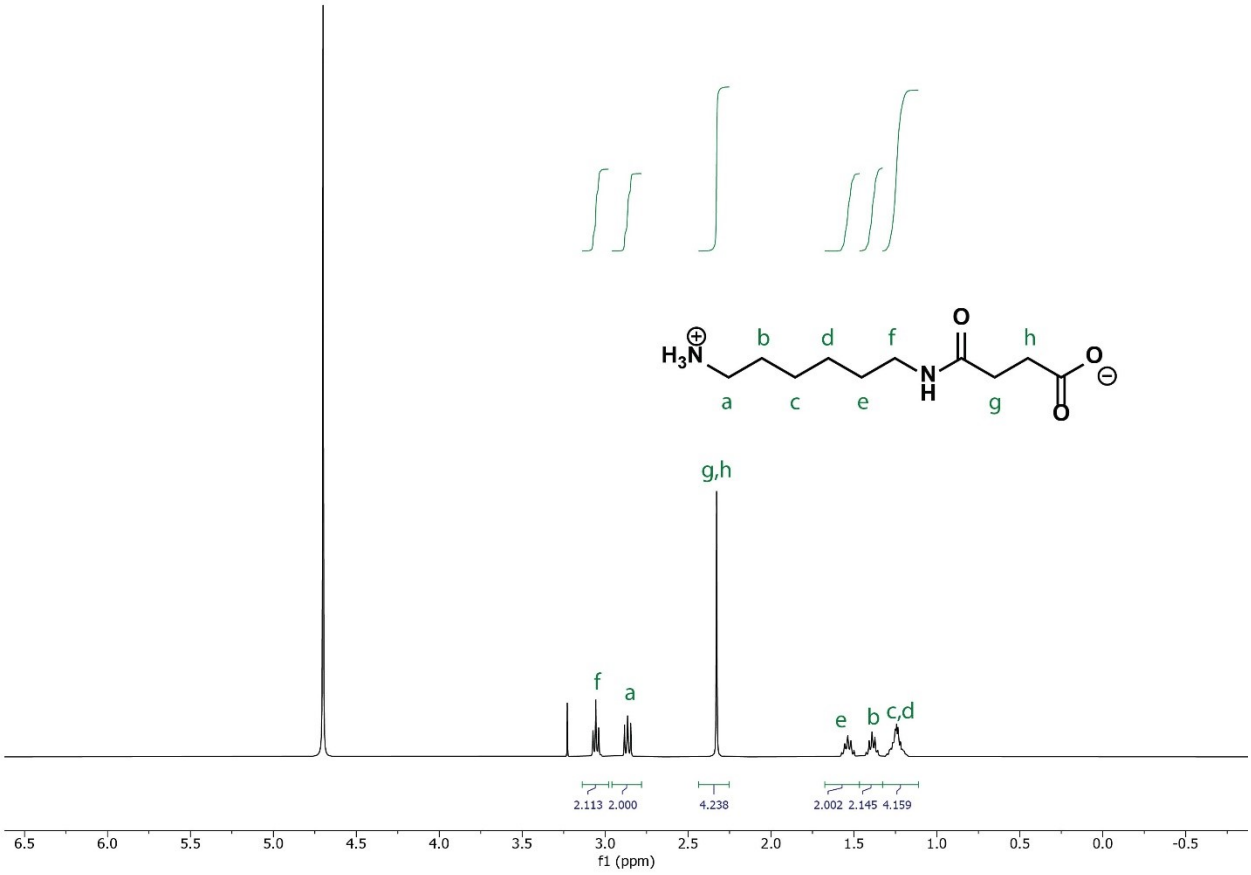

Figure S7. ^{1}H NMR spectrum of L1 collected in D_2O.

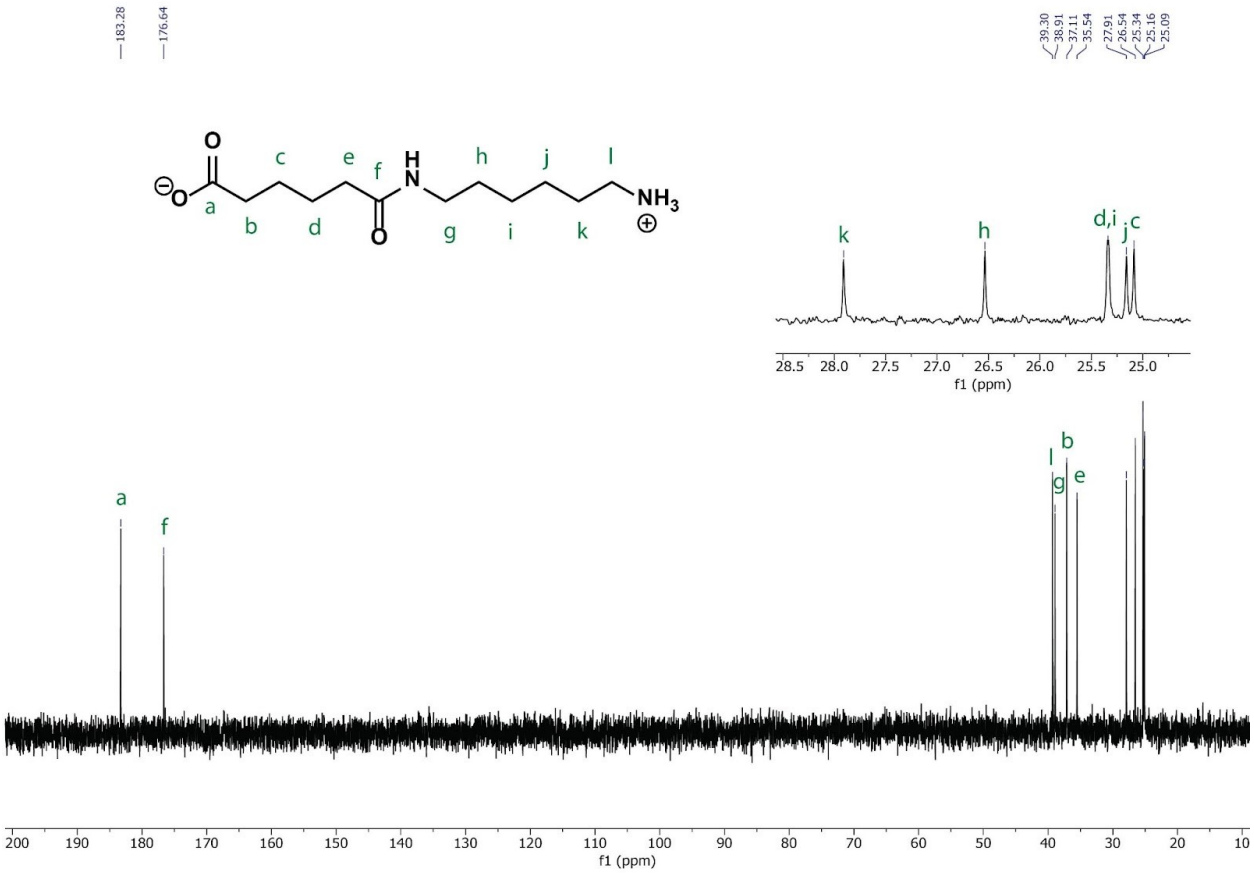

Figure S8. ^{13}C NMR spectrum of MA in D_2O.

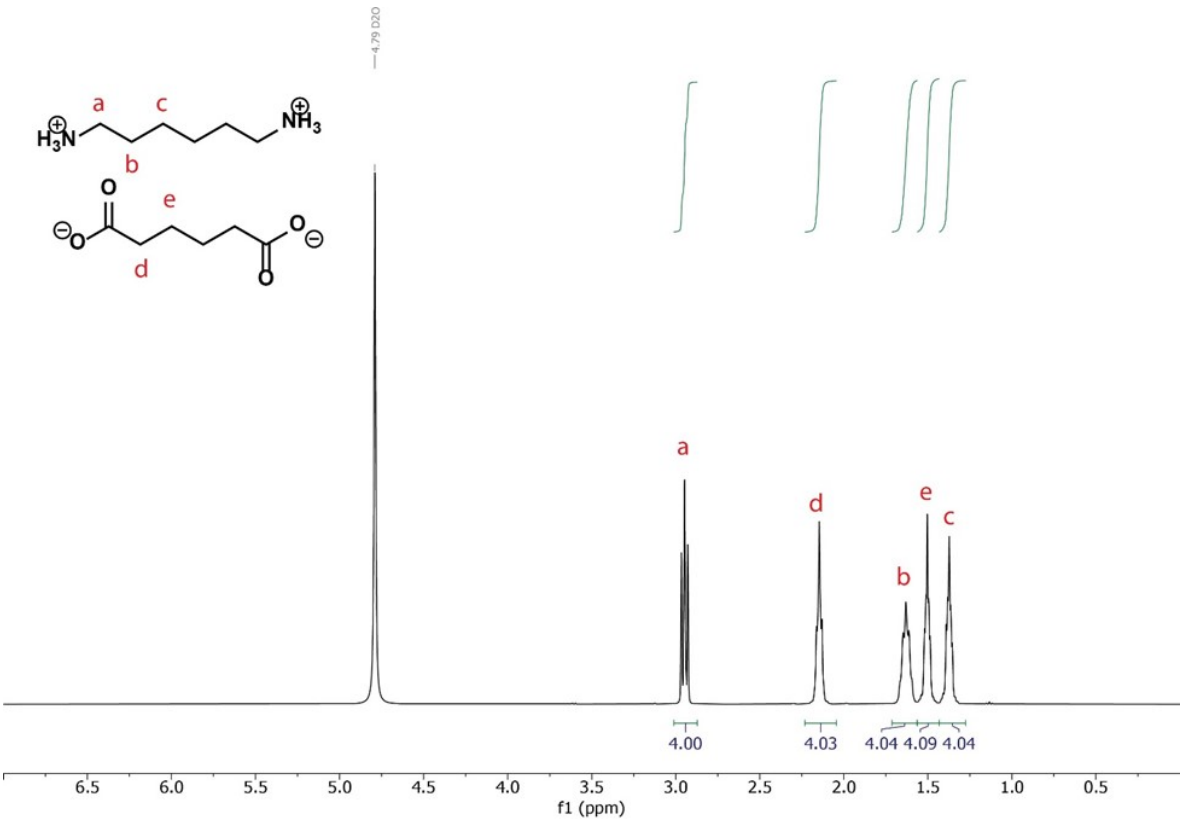

Figure S9. ^{1}H NMR spectrum of Nylon – 6,6 salt collected in D_2O.

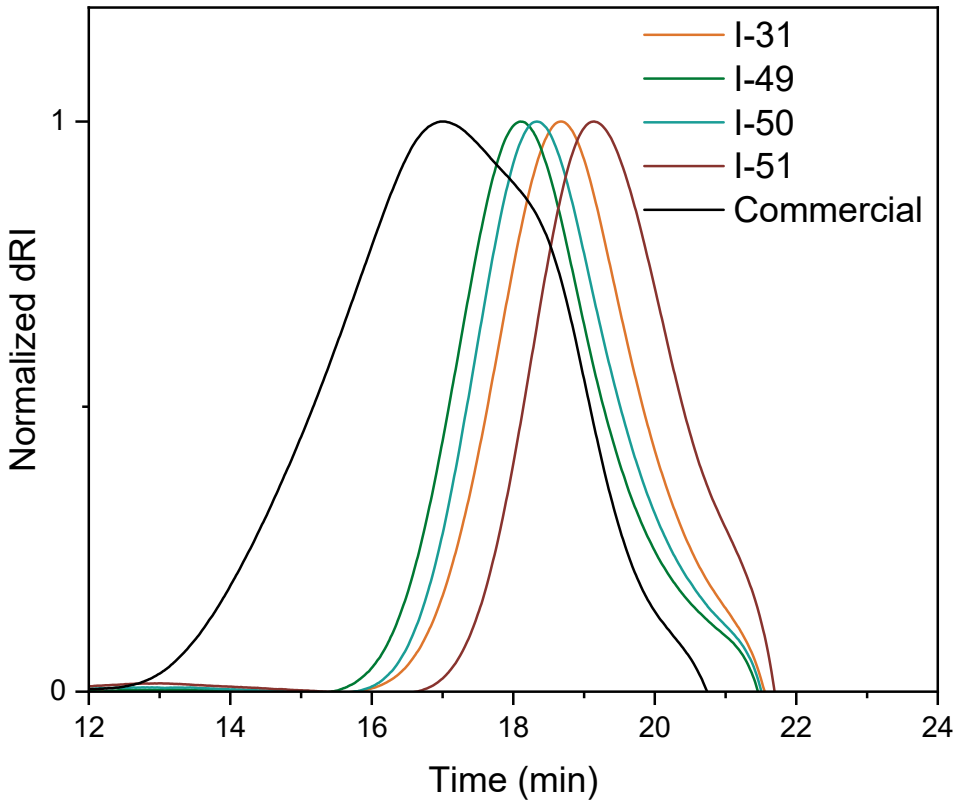

Figure S10. GPC data normalized to the peak maximum for Nylon – 6,6 .

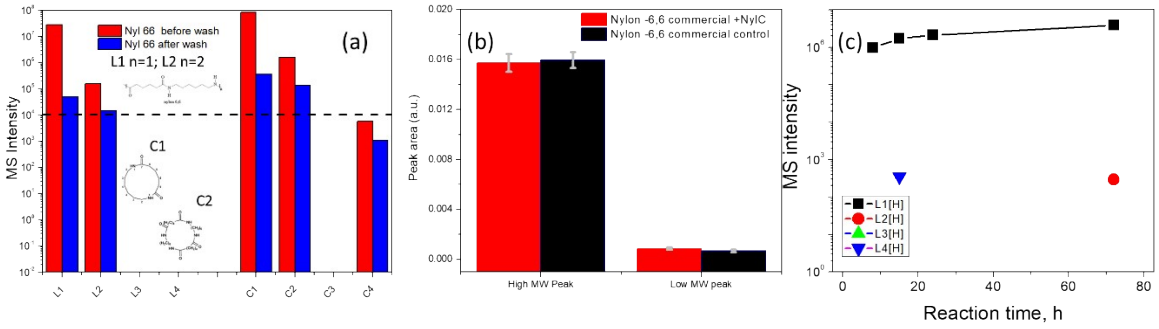

Figure S11. MS of commercial ball-milled Nylon – 6,6 a) before and after washing and c) after washing during the kinetic experiments with NylC b) Areas of high and low MWs peaks of SEC curve presented in Figure 1a

The statistical significance of the differences between samples and control for 0.00086 ± 0.0001 vs. 0.00068 ± 0.0001 (Low Mw peaks) and 0.01573 ± 0.00072 vs. 0.01596 ± 0.00063 (High MW peaks) was evaluated. The first comparison yielded a Z-score[1] of 1.28 and a p-value[1] (the standard normal distribution two-tailed test) of 0.2006, suggesting possible significance at the 80% confidence level. The second comparison resulted in a Z-score of 0.24 and a p-value of 0.8104, indicating no statistical significance, as the observed variation is likely due to random fluctuations.

Table S1 contains characteristics of all studied Nylon 66 samples

Sample	Mn (g/mol)	Mw (g/mol)	T_g (°C)	Tm(°C)	Enthalpy of melting (J/g)	Surface area (m^2/g)	Crystallinity (Xray %)	Density (g/cm^3)	Particle radius (µm)
Nylon 66_Com	35513	76347	57.1 ± 1.9	259.34	69.304	1.15	15.1	1.16±0.01	2.2
I31	2652	9092	44.4 ± 2.7	257.67	91.213	-	29.3	1.21±0.02	-
I49	4083	14277	50.3 ± 3.2	258.63	91.589	-	29.0	1.20±0.01	-
I50	3215	11251	47.4 ± 2.7	257.54	88.603	2.47	28.4	1.20±0.02	1.01
I51	1528	5121	43.5 ± 4.7	254.36	91.482	4.42	36.2	1.21±0.01	0.56

MD simulation for C1 and C2 substrates

In the experiment, C1 was not degraded by the enzyme, while **C2** was successfully degraded. To investigate the possible mechanism underlying this observation, we conducted molecular dynamics (MD) simulations (see Methods). Figure S12 shows snapshots of **C1** and **C2** with the enzyme in solution, illustrating the initial structures after the Steered Molecular Dynamics (SMD) simulation and their evolution during the subsequent 5 ns NPT simulation. The snapshots clearly demonstrate that CL2 remains near the catalytic residue, whereas **C1** moves away from the catalytic site. Figure S13 presents the tracked distance between the carbonyl carbon in amide group of the nylon substrate and the catalytic residue over the 5 ns simulation, along with snapshots of the substrates, providing further evidence of their differing behaviors.

Both C1 and C2 naturally exhibit rounded structures. During the dynamic simulation of **C2**, the substrate transitions into a more elliptical shape, as shown in Figure S13b(ii). This causes **C2** to momentarily shift out of the pocket but subsequently return closer to the catalytic residue, as shown in Figure S13b(iii). **C2**'s lateral region, which interacts with the enzyme pocket, narrows to fit the pocket's shape. A similar adaptation was observed with **L2**, as detailed in MD simulation part related to **L1** and **L2** substrates. In contrast, **C1** lacks significant interaction between its lateral part and the pocket. Although **C1** initially adjusts its shape similarly to **C2**, once it is pushed out of the

pocket, it is difficult to readjust due to high mechanical strain, making re-binding unfavorable. These observations suggest that the substrate's shape and mechanical strain play crucial roles in determining its binding preference with the enzyme.

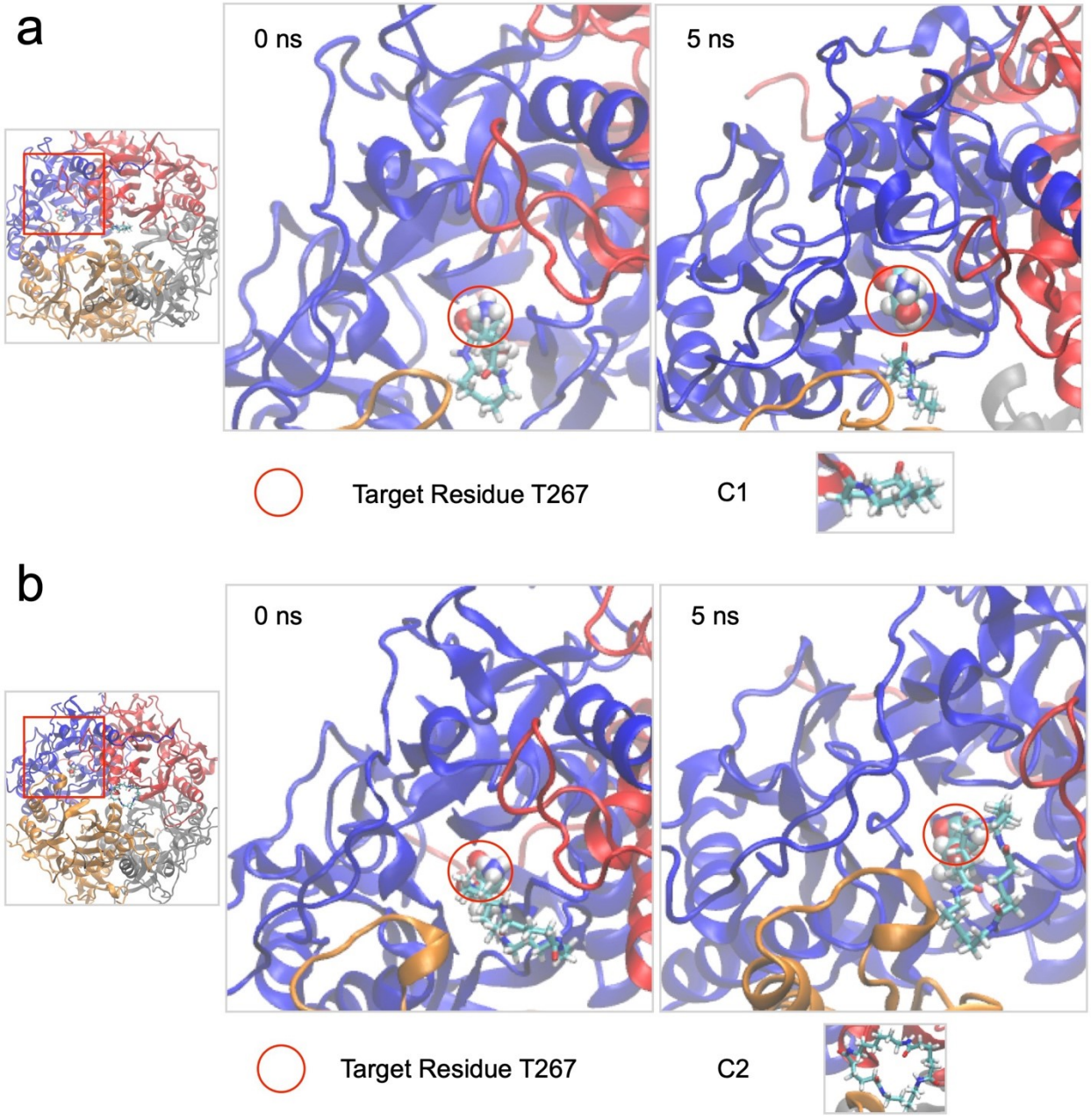

Figure S12. Snapshots of NylC-GYAQ and Nylon **C1** (**a**) and **C2** (**b**) during the simulations: (left) Initial positions and shapes of Nylon substrates. (middle) After pulling carbonyl carbon towards T267. (right) After 5ns of MD simulations.

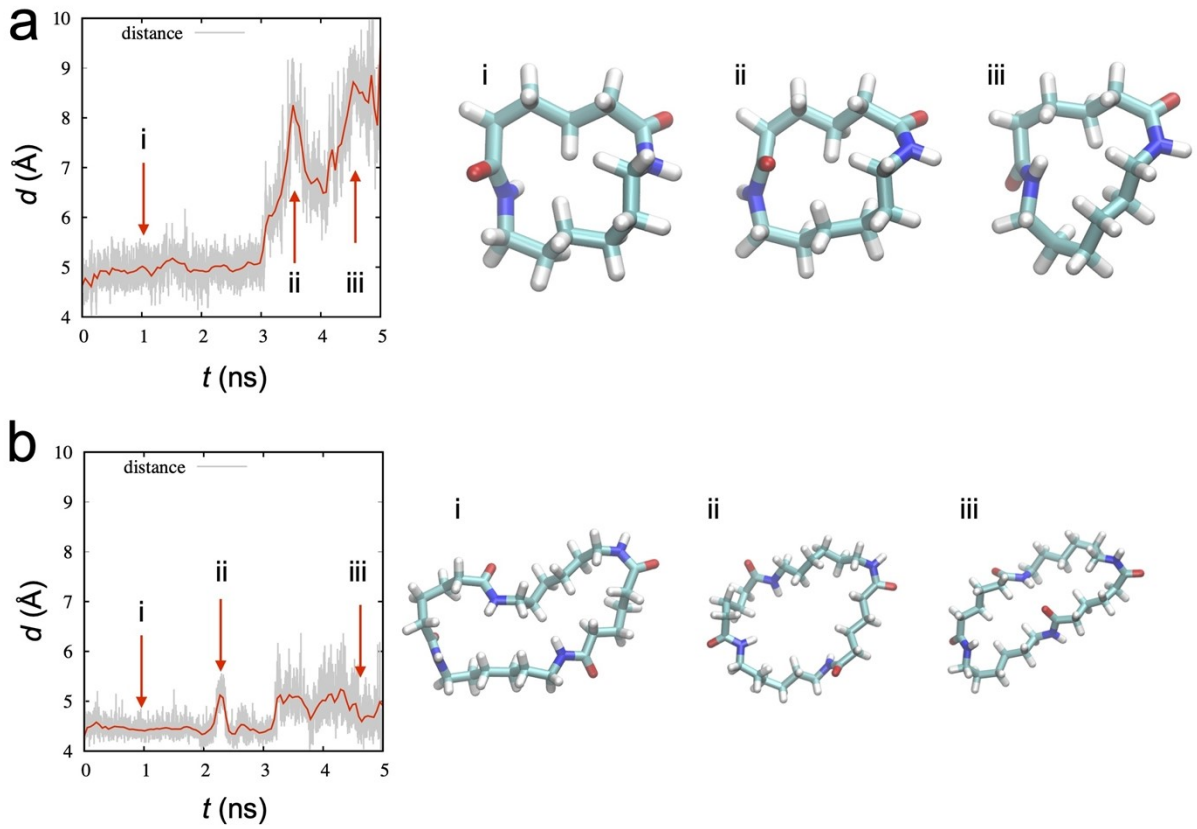

Figure S13. The time evolution of the distance (*d*) between the catalytic residue T267 of NylC-GYAQ and the carbonyl carbon of Nylon-6,6 cyclic monomer (**a**) and dimer (**b**). Each panel includes snapshots of Nylon chains at specific time points labeled as i, ii, and iii.

MD simulations of L1 and L2 substrates

We further conducted simulations with **L1** and **L2**, similar to those described in MD simulation for **C1** and **C2** substrates, with the results shown in the snapshots in Figures S14 and S15. Both **L1** and **L2** were stabilized near the binding pocket. For **L2**, interactions with the NylC-GYAQ pocket caused the nylon substrate to adopt a bent or cyclic conformation, stabilizing near the catalytic residue, as shown in Figure S15b. Additionally, we observed that the chain ends of the substrate tended to interact with each other, contributing to its stabilization. This observation aligns with the behavior of C2, where the deep and narrow pocket in NylC-GYAQ induces the substrate to deform or bend into a more elliptical shape.

In contrast, **L1** exhibits different behavior in its conformation. Initially, the SMD simulation brought the carbonyl carbon in the amide group close to the catalytic residue, causing **L1** to adopt a rounded shape. However, **L1** later straightened and remained stretched. While **L1** appears stable near the catalytic residue, it maintains a greater distance compared to **L2** due to this stretched conformation. This suggests that **L1** may act as an inhibitor near the catalytic site without undergoing hydrolysis, despite having an amide group capable of hydrolysis. The differences in behavior between **L1** and **L2** can be attributed to the short persistence length of approximately 0.6 nm reported for nylon polymers.[2] Given **L1**'s length of about 1.4 nm, it is more likely to maintain a straighter conformation, unlike **L2**, which is twice as long and more prone to bending.

Given that a bent substrate shape is essential for both **L2** and **C2** to stabilize near the catalytic residue, the NylC enzyme likely functions as an exo-cleaving enzyme for soluble single chains. This is because, mechanically, bending becomes increasingly difficult at the center of the nylon polymer as the chain length increases.

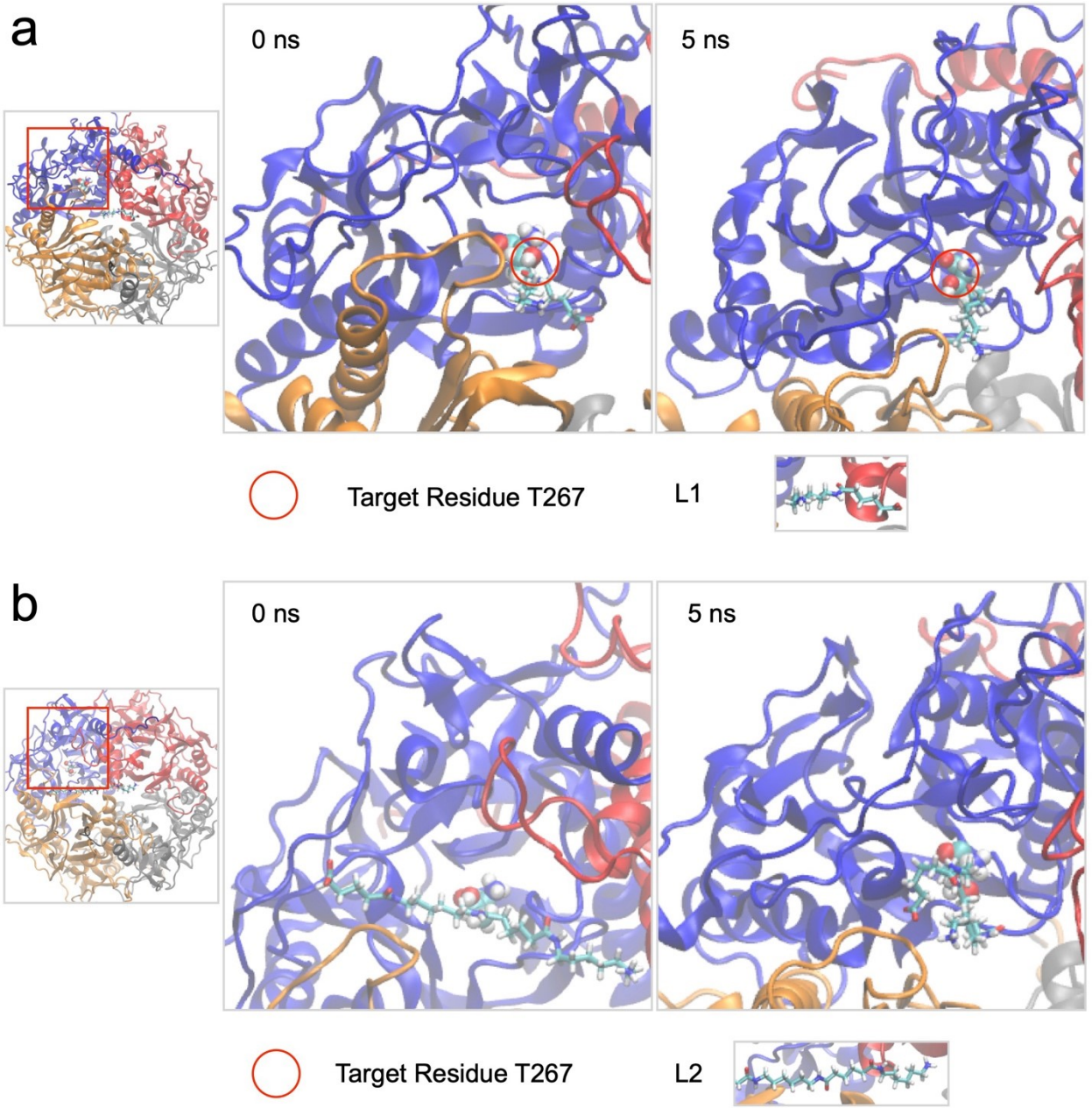

Figure S14. Snapshots of NylC-GYAO and Nylon **L1** (**a**) and **L2** (**b**) during the simulations: (left) Initial positions and shapes of Nylon substrates. (middle) After pulling carbonyl carbon towards T267. (right) After 5ns of MD simulations.

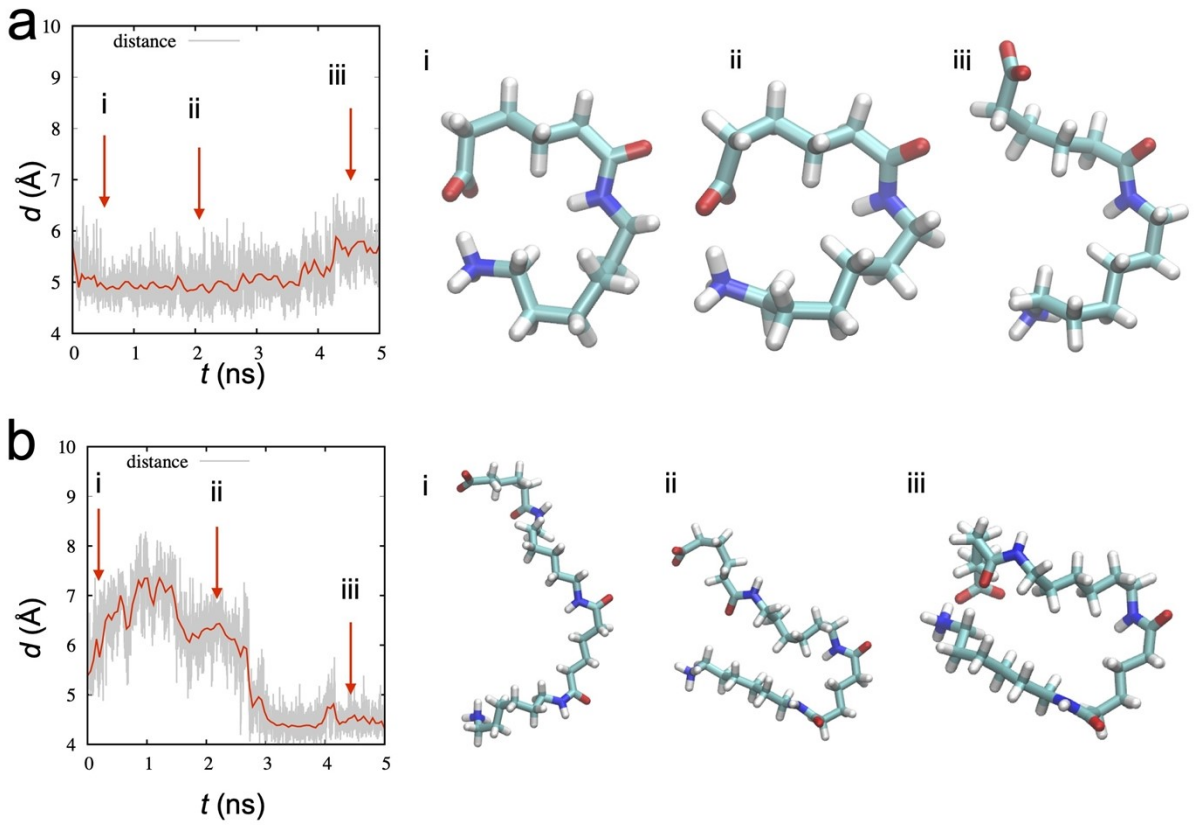

Figure S15. The time evolution of the distance (*d*) between the catalytic residue T267 of NylC-GYAQ and the carbonyl carbon of Nylon-6,6 linear monomer (**a**) and dimer (**b**). Each panel includes snapshots of Nylon chains at specific time points labeled as i, ii, and iii.

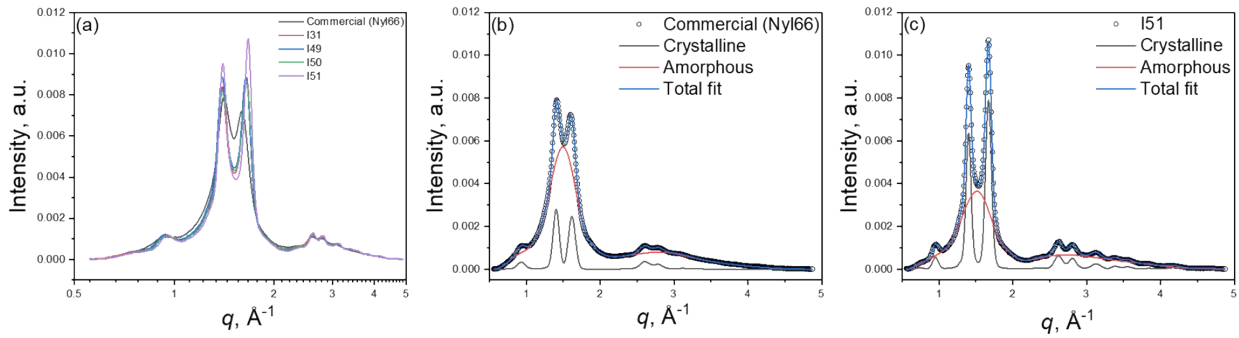

Figure S16. a) WAXS spectra of studied Nylon -6,6 samples, examples of fitting for b) commercial Nylon – 6,6 and (c) I51 sample

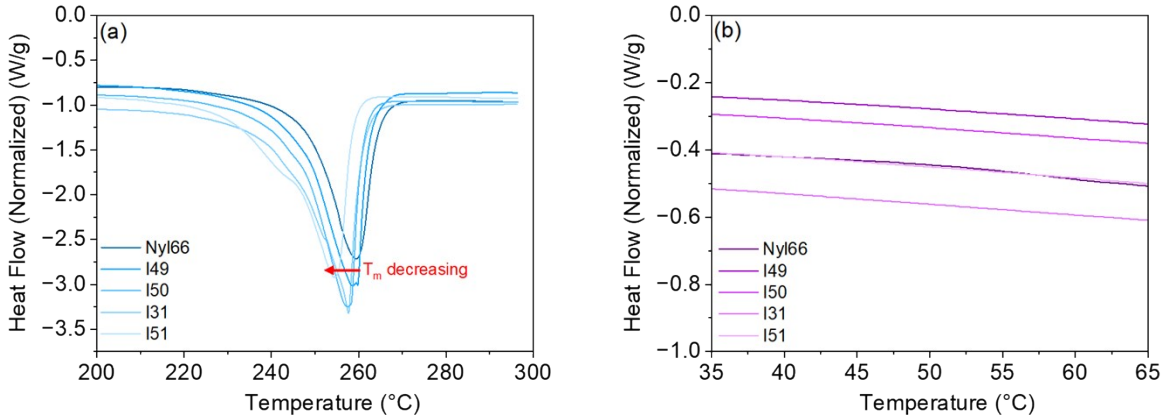

Figure S17. a) Melting temperature of Nylon – 6,6 samples with varied molecular weights. The enthalpy of melting was obtained through the integration of the valley area. b) DSC plot of studied Nylon-6,6 samples, of which the range was used to extract the glass transition temperature using the TA Instruments Universal Analysis 2000 software.

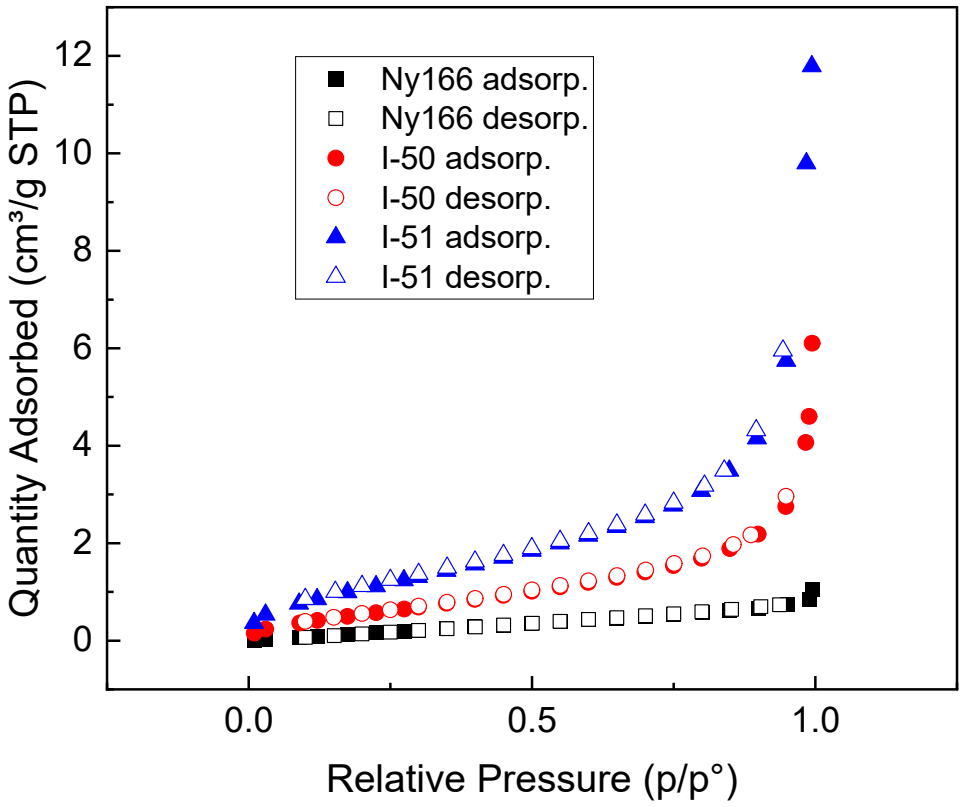

Figure S18. BET data for studied Nylon – 6,6

Details of the model

Each particle in the model represents an aggregate of polymer chains. Some polymer chains are located on the surface of the particle, with their ends accessible to enzymes in the solution, while others are inside the particle, where enzyme access is restricted (see Figure S11). We also assume two scenarios for hydrolysis: (i) enzymes in the solution that associate and dissociate with surface-confined chain ends, and (ii) enzymes tightly attached to the chain. In this case, the total yield, Y_{total}, can be expressed as superposition of two yields

$$Y_{total} = Y_{a\leftrightarrow d} + Y_c \tag{S1}$$

where $Y_{a\leftrightarrow d}$ is the yield provided by enzymes from the solutions which can attach and detach to the polymer chain located at the surface of the particle, Y_c is the yield provided by enzymes tightly sitting on the polymer chains, and its dependence derived from experimental data.

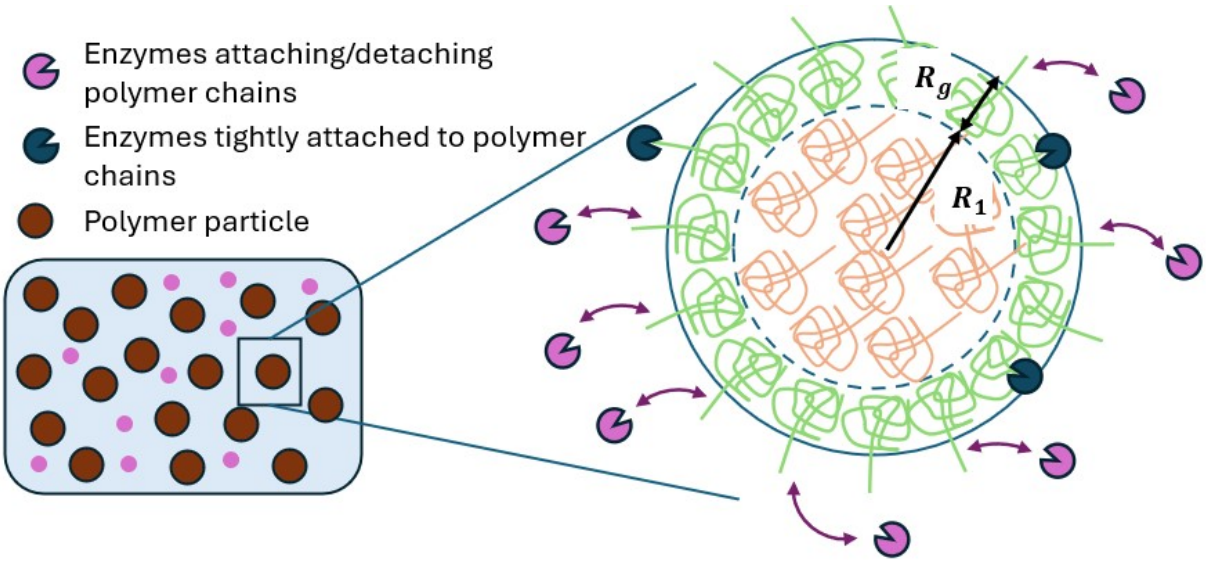

Figure S19. Schematic representation of the suspension with enzymes and polymer particles. Each particle presents an aggregate of polymers chains. The polymer chains in the particle can be divided in two types: i) Polymer chains at the surface of the particle (marked by green color), with the ends accessible by enzymes in the solution and ii) polymer chains inside of the particle (marked by orange color), with restricted access by enzymes from solutions.

The thickness of the surface layer of the polymer particle is assumed to be equal to the gyration radius of the polymer coil, ^{R_g}. If we denote the total number of polymer chains per particle as $^{N_{p,1}}$, then we can write that the volume of the polymer particle, ^{V_p}, is equal to

$$V_p = \frac{4\pi}{3}(R_1 + R_g)^3 = \frac{4\pi}{3}(R_g)^3 N_{p,1} \tag{S2}$$

where ^{R_1} is the distance from the center of the particle to the surface area (see Figure S11). From Eq.(S2) we have

$$R_1 = R_g(N_{p,1}^{\frac{1}{3}} - 1) \tag{S3}$$

Then the volume of the surface layer, ^{V_s}, can be presented as follows

$$V_s = V_p - \frac{4\pi}{3}(R_1)^3 = V_p - \frac{4\pi}{3}(R_g)^3\left(N_{p,1}^{\frac{1}{3}} - 1\right)^3 \approx (N_{p,1} \gg 1) \approx 3V_p N_{p,1}^{-\frac{1}{3}} \tag{S4}$$

The yield $Y_{a\leftrightarrow d}$ depends on the total number of the particle in the solution, $N_{particle}$, and the probability that the polymer chain is located on the surface of the particle, which is equal to $N_{p,1} * V_s/V_p$. In this case, we have

$$Y_{a\leftrightarrow d} \propto N_{particle} * N_{p,1} * \frac{V_s}{V_p} = 3N_{particle} * N_{p,1}^{\frac{2}{3}} \quad \text{(S5)}$$

Using the expression for the total surface area of the particles we have

$$S_{total} = N_{particle} * 4\pi(R_1 + R_g)^2 = N_{particle} * 4\pi R_g^2 N_{p,1}^{\frac{2}{3}} \quad \text{(S6)}$$

we can express the yield in Eq.(S5) as follows

$$Y_{a\leftrightarrow d} \propto \frac{S_{total}}{R_g^2} \quad \text{(S7)}$$

Taking into account that $R_g \propto \sqrt{Mw}$, where Mw is the molecular weight of the polymer chain we can write the final expression for the first mechanism as

$$Y_{a\leftrightarrow d} \propto \frac{S_{total}}{Mw} \quad \text{(S8)}$$

---

[1] McClave, James T., P. George Benson, and Terry Sincich. *Statistics for business and economics*. Pearson Education, 2008.

[2] Lukasheva, N. V., Tolmachev, D. A., Nazarychev, V. M., Kenny, J. M. & Lyulin, S. V. Influence of specific intermolecular interactions on the thermal and dielectric properties of bulk polymers: atomistic molecular dynamics simulations of Nylon 6. *Soft Matter* **13**, 474-485 (2017).